Journal of Catalysis **197,** 244–250 (2001)
doi:10.1006/jcat.2000.3096, available online at http://www.idealibrary.com on IDEAL®

Decomposition of PF_3 on Ni(755) and Coadsorption with Ethylcyclohexane: Comparing the Results of PF_3 with CO

Hideo Orita,[1] Hiroshi Kondoh, and Hisakazu Nozoye

National Institute of Materials and Chemical Research, Tsukuba, Ibaraki 305-8565, Japan

Received February 25, 2000; revised August 17, 2000; accepted October 25, 2000; published online December 21, 2000

Temperature-programmed desorption spectra for exposure of PF_3 on Ni(755) are characterized by two desorption features around 350 and 650 K. The lower temperature feature is assigned to the molecular desorption and the higher one to the recombinative desorption of PF_3 fragments, respectively. The results suggest that the decomposition of PF_3 occurs at the step sites but not on the terrace of Ni(755). Coadsorbed PF_3 inhibits the decomposition of ethylcyclohexane almost completely and the inhibiting effect of PF_3 is more effective than that of CO. We can obtain the same decomposition starting temperature (the temperature where an adsorbed hydrocarbon starts to decompose) of ethylcyclohexane by using the inhibiting effects of PF_3 and CO. © 2001 Academic Press

Key Words: **PF_3; decomposition; CO; Ni(755); coadsorption; TPD.**

1. INTRODUCTION

PF_3 has received some attention from surface chemists as a probe molecule to study properties of metal surfaces due to the similarities in its bonding to transition metals to that of CO: i.e., σ donation from its lone pair electrons (nonbonding orbital on phosphorous) to an empty orbital of the metal and π back-donation from metal *d* orbitals to the antibonding orbital (7*e*) of the molecule (the 7*e* orbital consists of *p* and *d* orbitals on the phosphorous atom). Nitschke *et al.* (1) have used ultraviolet photoelectron spectroscopy (UPS) and low-energy electron diffraction (LEED) to study properties of PF_3 on metal surfaces. They have observed that a saturation coverage of PF_3 on Ni(111) produces a $p(2 \times 2)$ LEED pattern, which is unstable in the electron beam, and that PF_3 is thermally stable below 400 K. Alvey and Yates (2) have indicated from their ESDIAD (electron-stimulated desorption ion angular distribution) experiments that PF_3 is adsorbed on Ni(111) at atop sites and is azimuthally oriented so that the individual P–F bonds are directed over neighboring Ni atoms. Dippel *et al.* (3) have determined the adsorption structure of PF_3 on Ni(111) by the use of photoelectron diffraction; PF_3 occupies an atop site with a P–Ni nearest neighbor distance of 2.07 ± 0.03 Å. Unlike CO, which occupies different adsorption sites (for example, three-fold, two-fold, and one-fold coordination sites coexist on Ni(111)), PF_3 has no ability for bridging coordination independent of coverage.

The structure and reactivity of coadsorbed species are topics of considerable interest and importance. Various coadsorption systems have been studied on many well-defined metal surfaces in the past to reveal the interaction between coadsorbates (e.g., alkali metal and CO (4), CO and hydrogen (5), CO and benzene (6), CO and ethene (7), Bi and hydrocarbons (8), CO and NH_3 (9), and K and methylcyclohexane (10)). The influence of several coadsorbates on the overlayer structure of PF_3 on Pt(111) has been studied already (11). However, the coadsorption system of PF_3 and a hydrocarbon has scarcely been investigated.

The coadsorption of CO and unsaturated hydrocarbons has already been studied by many researchers (6, 7), and it has been revealed that the coadsorption of CO induces ordered structures that cannot be observed in each separate adsorption. Coadsorbed CO usually acts as a site blocker for dissociation and reduces decomposition probability of hydrocarbons considerably.

We have previously investigated the coadsorption of saturated hydrocarbons and CO on Ni(755), which is denoted [6(111) × (100)] in step notation, by means of temperature-programmed desorption (TPD), changing the coverages of the adsorbates carefully, and have found a novel promoting effect of coadsorbed CO on the decomposition of "low-reactivity" hydrocarbons, which decompose little during a TPD run. For example, the coadsorbed CO at a coverage around 0.2 ML (1 ML = one molecule or atom per exposed surface Ni atom) promoted the decomposition of cyclohexane up to about 10 times (12). For "high-reactivity" hydrocarbons such as cycloheptane, which decompose completely at their low coverages without desorbing parent molecules during the TPD run, coadsorbed CO at a coverage below ca. 0.2 ML does not suppress the high decomposition probability of the hydrocarbons (13). When CO coverage increases, coadsorbed CO displaces a hydrocarbon from the first layer

[1] To whom correspondence should be addressed. Fax: +81-298-61-4504; Phone: +81-298-61-4527. E-mail: orita@nimc.go.jp.

0021-9517/01 $35.00

on the surface to a second layer on CO, and the decomposition of low-reactivity as well as high-reactivity hydrocarbons is suppressed. In that paper, we have also presented a method to determine the decomposition starting temperature of high-reactivity hydrocarbons (i.e., the temperature where an adsorbed hydrocarbon starts to decompose) by making use of the change in TPD spectra (peak area and shape) after preflash, quenching, and postdosing of CO.

We have studied the desorption behavior of PF_3 and the coadsorption of PF_3 with saturated hydrocarbons on Ni(755) by TPD. The main motivation for this study was to compare the effect of PF_3 on the decomposition of hydrocarbons with that of CO because these two molecules show a similar adsorption mechanism on metals. Results for the decomposition of ethylcyclohexane are presented as a representative case for high-reactivity hydrocarbons to show whether or not the extent of inhibiting effects of coadsorbates influences the determination of the decomposition starting temperature of a hydrocarbon. The results show that PF_3 inhibits the decomposition of ethylcyclohexane more effectively than CO and that the same decomposition starting temperature of ethylcyclohexane is obtained by using the inhibiting effects of PF_3 as well as CO.

2. EXPERIMENTAL

All experiments were conducted in a stainless steel ultrahigh vacuum system equipped with a single-pass CMA for Auger electron spectroscopy (AES), four-grid LEED optics, a quadrupole mass spectrometer for TPD, and an ion gun for cleaning. The base pressure was less than 1×10^{-10} Torr (1 Torr = 133.3 Pa). A disk-shaped Ni(755) crystal (ca. $\Phi 8 \times 1$ mm) was heated resistively and cooled down to 90 K. The sample temperature was measured by a chromel–alumel thermocouple spot-welded to the edge of the crystal. The Ni(755) surface was cleaned by Ar-ion sputtering followed by annealing to 1080 K. Cleanliness and ordering of the surface were checked by AES and LEED.

Exposure of gases on the surface was performed using a gas doser, which was composed of a glass capillary array. The exposure was controlled by varying dose time and back pressure of the doser (usually 1×10^{-4} Torr, which was not corrected for ion gauge sensitivity to various gases). TPD experiments were carried out with a linear heating rate of 10 K/s controlled by a personal computer. Four mass signals were monitored simultaneously in a single experiment, and the data were stored in the computer. The coverage of adsorbed CO relative to a surface Ni atom was determined from the integrated mass intensity of the TPD peak, assuming that the saturation coverage at 348 K is 0.5 ML, which has already been established for Ni(111) (the terrace of Ni(755)) at 300 K (see, for example, Ref. (14)). Under the present experimental conditions, the saturation coverage of CO at 348 K (i.e., 0.5 ML) was accomplished at a dose time of 50 s.

We could determine the mass sensitivity factor for hydrogen from TPD for H_2 adsorption. Hydrogen molecules adsorb dissociatively on Ni(755) and the saturation coverage of an adsorbed hydrogen atom is 1 ML (15). The amount of decomposed ethylcyclohexane was calculated from that of evolved hydrogen. We could calibrate also the mass sensitivity factor for ethylcyclohexane by using the TPD peak areas of both hydrogen and ethylcyclohexane since the mass balance between hydrogen and ethylcyclohexane was conserved in the cases of coadsorption with PF_3 or CO. Thus, the amounts of decomposed ethylcyclohexane were calculated by using this sensitivity factor. Although all the TPD spectra for hydrogen were not corrected for the hydrogen adsorption from residual gas, the amount of hydrogen adsorbed from residual gas was usually much smaller than that from the decomposition of ethylcyclohexane and could be subtracted easily from the total amount of desorbed hydrogen except when mentioned in the text.

Ethylcyclohexane was purchased and purified by at least five freeze–pump–thaw cycles. The hydrogen, PF_3, and CO were research-grade purity and used without further purification. Mass spectra of all the gases were checked for purity after admission into the ultra-high vacuum chamber.

3. RESULTS AND DISCUSSION

3.1. TPD Spectra for PF_3

For Ni(111), Alvey and Yates (2) have measured TPD spectra of PF_3 adsorbed at 85 K. They have reported that the coverage of PF_3 does not saturate at 85 K and that a single peak at 405 K, which broadens to lower temperatures, appears at first and a broad high-temperature desorption feature extending up to 1000 K is also observed for a larger exposure. Furthermore, they have observed a $p(2 \times 2)$ LEED pattern after exposing Ni(111) to 2.6×10^{15} PF_3 cm^{-2} and then briefly flashing the crystal to 275 K. The $p(2\times2)$ pattern is consistent with a surface coverage of 0.25 ML. With this as a reference point, they estimate PF_3 coverages from the PF_3 exposures.

Considering the above results, we have investigated the adsorption and decomposition of PF_3 on Ni(755) by TPD and used a rather higher adsorption temperature of 273 K to avoid multilayer adsorption. Figures 1a and 1b show a set of TPD spectra of PF_3 (PF_2^+, $m/e = 69$) and mass integrated intensities of PF_2^+ ($m/e = 69$) and PF_3^+ ($m/e = 88$), respectively. We mainly used $m/e = 69$ to monitor PF_3 since it has the highest intensity in the cracking pattern of PF_3 and we assured that it showed behavior identical to that of the parent peak ($m/e = 88$). As shown in the inset to Fig. 1b, the intensity ratio of two signals at $m/e = 69$ and 88 was constant at 0.2 ± 0.05. The scatter of the data came from the low

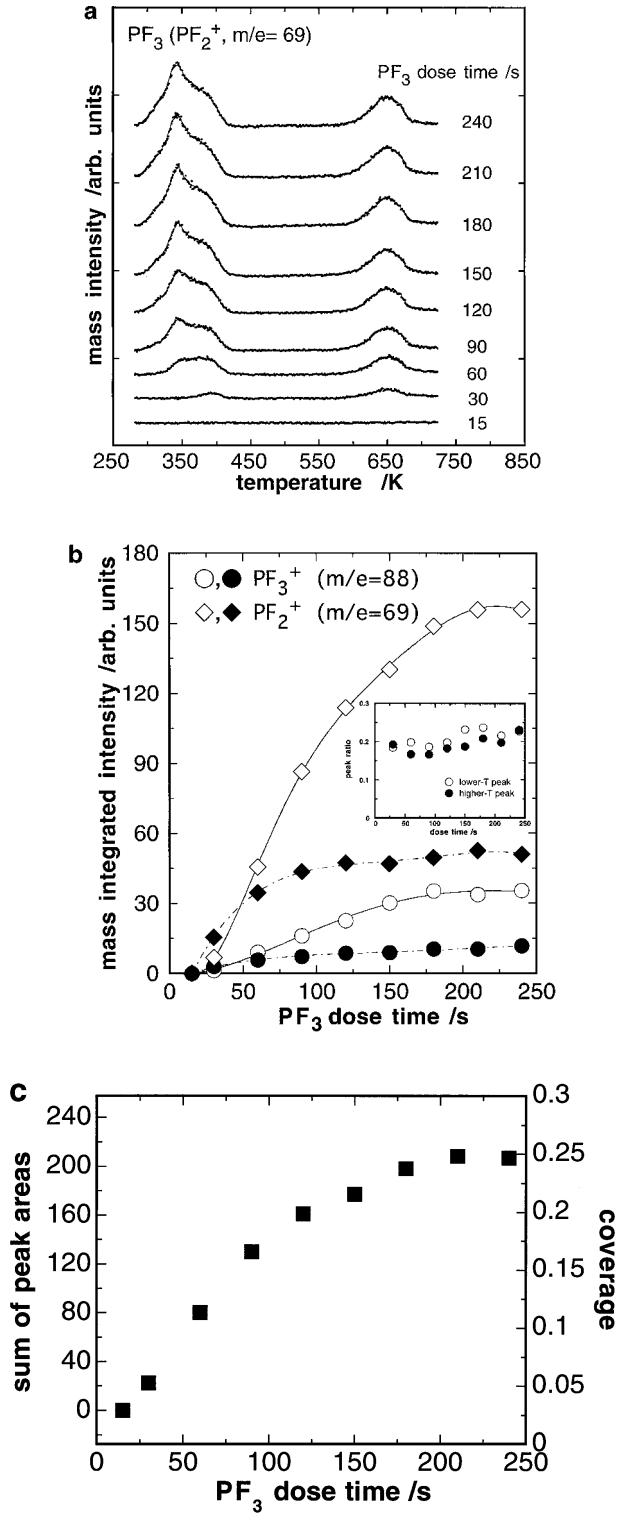

FIG. 1. (a) TPD spectra for PF_3 (PF_2^+, $m/e = 69$) adsorbed on Ni(755) at 273 K as a function of PF_3 dose time. (b) Variations in peak areas of PF_2^+ ($m/e = 69$) and PF_3^+ ($m/e = 88$) with PF_3 dose time. Open and filled symbols indicate the molecular desorption and the recombinative desorption of PF_3 fragments, respectively. The inset shows the intensity ratio of the two signals at $m/e = 69$ and 88. (c) Variation in the sum of the peak areas of the two desorption features of $m/e = 69$ with PF_3 dose time. The indicated lines are only guides for the eyes.

intensity of the parent peak. No gas-phase products other than PF_3 were detected by TPD. The TPD spectra for PF_3 were characterized by two desorption features around 350 and 650 K. The higher temperature peak grew faster than the lower one and was saturated by a dose time of 90 s (cf. Fig. 1b). Its peak position remained almost unchanged at 648–654 K independent of dose time. The lower temperature peak appeared at 393 K at a dose time of 30 s. This peak grew broader and shifted to lower temperature (ca. 385 K) with an increase of dose time. After a dose time of 60 s, a new shoulder peak around 350 K appeared and increased in intensity with further exposure. The total area of the lower temperature peaks was saturated by a dose time of 210 s.

Alvey and Yates (2) have measured similar TPD spectra after adsorption of PF_3 on Ni(111) followed by electron bombardment and observed that the lower temperature desorption feature decreases in intensity while the higher one increases with increasing electron fluence. They have assigned the higher temperature peak around 650 K to the recombination peak of PF_3 fragments such as P and F, which are produced by electron bombardment. When the above assignments of Alvey and Yates (2) were used, the lower-temperature desorption feature and the higher one in Fig. 1a of the present work were assigned to the desorption of undecomposed PF_3 and the recombination peak of PF_3 fragments, respectively. The ratio of the saturation peak area of the lower temperature desorption feature to that of the higher one was about 3 : 1. It is clear from Fig. 1b that the sites for the higher temperature desorption feature were already saturated with PF_3 by a dose time of 90 s while only about half the sites for the lower one were occupied with PF_3. The most appropriate candidate for the sites for the decomposition of PF_3 is the step of Ni(755) because the higher temperature desorption feature around 650 K was not observed for Ni(111) without electron bombardment.

LEED measurements were performed at submonolayer coverages of PF_3. No additional LEED pattern due to an ordered overlayer was observed, but only a bright background was seen. Although we could not observe a clear LEED pattern, we tentatively estimated the coverage of PF_3 from the TPD peak area on the basis of the following considerations. When a PF_3 molecule is placed on an atop site to form the $p(2 \times 2)$ structure extending from the step edge atom, the coverage of PF_3 on Ni(755) becomes also 0.25 ML, which has already been established for Ni(111) (2). Figure 1c shows variations in the sum of peak areas of two desorption features of PF_2^+ ($m/e = 69$) with PF_3 dose time. The behavior of the peak area was similar to that observed for adsorption of PF_3 on Ru(001) and Cu/Ru(001) through mobile precursor states (16) (i.e., linear increase in shorter dose times up to 90 s and gradual increase to saturation). On Ni(755), however, no desorption of PF_3 was observed at a short dose time of 15 s, suggesting that all the adsorbed PF_3 decomposed at this dose time. In fact, AES revealed that

phosphorus remained on the surface after TPD measurements, but we could not carry out a quantitative measurement of PF_3 coverage by AES since it was difficult to avoid electron-stimulated desorption and decomposition of PF_3 by the electron beam of our AES system. It is probably reasonable to estimate the amount of PF_3 adsorbed at the dose time of 15 s, which was relative to the TPD peak area, from the extrapolation of the linear relationship in a shorter dose time region and to assume that the sum of this extrapolated value and the saturation TPD peak area should correspond to a saturation coverage of 0.25 ML. With this as a reference point, PF_3 coverages could be estimated from the TPD peak areas, as shown in the right axis of Fig. 1c. Thus, the saturation coverages of the lower temperature desorption feature and the higher one were estimated to be ca. 0.17 and 0.05 ML, respectively. The coverage of PF_3 adsorbed on the terrace in the $p(2 \times 2)$ structure was two-thirds of 0.25 ML and was equal to the saturation coverage of the lower temperature desorption feature, suggesting that PF_3 adsorbed on the terrace desorbed without decomposition and that the decomposition of PF_3 occurred mainly at the step sites. At a dose time of 90 s when the higher temperature peak was saturated and that of 15 s when no desorption was observed (cf. Fig. 1a), for example, the total coverages of PF_3 would correspond to ca. 0.17 and 0.03 ML, respectively, when the above estimation was used.

3.2. *Coadsorption of Ethylcyclohexane with PF_3 or CO*

We have investigated the coadsorption of PF_3 and saturated hydrocarbons by TPD, changing the coverages of the adsorbates carefully. In this paper, results for the coadsorption of PF_3 and ethylcyclohexane are presented as an example for high-reactivity hydrocarbons to compare the effect of PF_3 on the decomposition of hydrocarbons with that of CO. TPD spectra of ethylcyclohexane were very similar to those of cycloheptane reported previously (13). For short dose time (<50 s), only hydrogen was detected. When the dose time was increased, the desorption of ethylcyclohexane began to appear at 253 K. This peak grew and shifted to 240 K upon further increases in dose time and was saturated at the dose time of 240 s (the saturation coverage of this peak was estimated to be 0.05 ± 0.01 ML by using the mass sensitivity factor of ethylcyclohexane). This state could be assigned to the desorption of molecularly adsorbed ethylcyclohexane (monolayer desorption). For a longer dose time (>180 s), another sharp peak appeared around 160 K before the saturation coverage of ethylcyclohexane adsorbed molecularly was reached. This sharp peak shifted to a little higher temperature (from 158 to 162 K in our experiments) and grew continuously with exposure without saturation. This peak was attributed to a condensed multilayer of ethylcyclohexane.

Figures 2a and 2b display the desorption of hydrogen ($m/e = 2$) and ethylcyclohexane ($C_4H_7^+$, $m/e = 55$), respectively, after dosing various amounts of PF_3 to clean Ni(755) at 123 K followed by exposure of a fixed amount of ethylcyclohexane (60-s dose time). The dependence of TPD peak areas of PF_3, H_2, and ethylcyclohexane on a PF_3 dose time is shown in Fig. 3. The reverse dosing sequence (i.e., ethylcyclohexane exposure followed by dosing PF_3) gave similar results to those in Figs. 2 and 3, which indicated pre-adsorbed PF_3 did not inhibit the adsorption of ethylcyclohexane greatly and vice versa. We used $m/e = 55$ to monitor ethylcyclohexane since it had the highest intensity in the cracking pattern of ethylcyclohexane and we assured that its behavior was the same as that of the parent peak ($m/e = 112$). No gas-phase products other than PF_3, hydrogen, and ethylcyclohexane were detected by TPD in

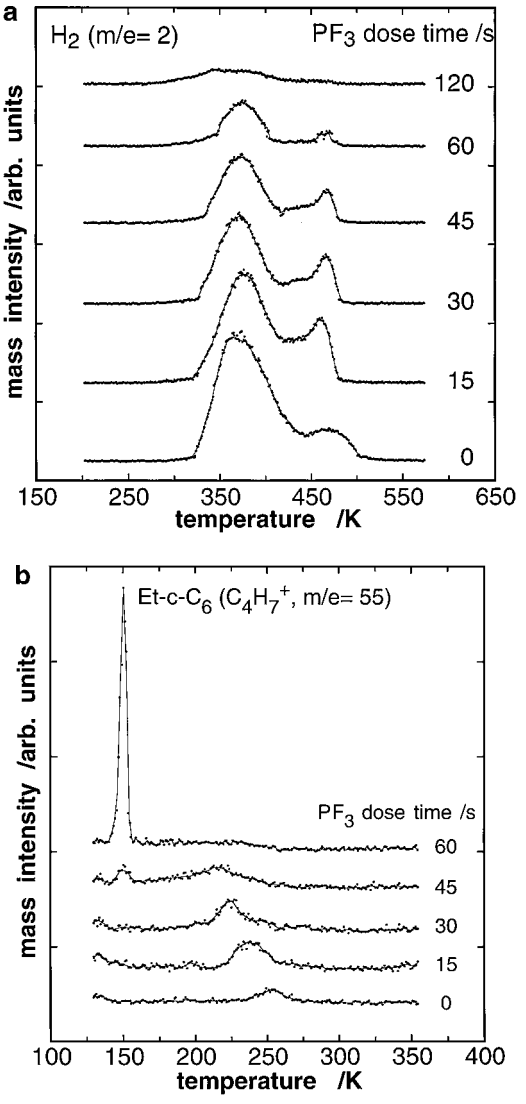

FIG. 2. Variations of TPD spectra for (a) hydrogen ($m/e = 2$) and (b) ethylcyclohexane ($C_4H_7^+$, $m/e = 55$) with PF_3 dose time. PF_3 was predosed to clean Ni(755) at 123 K and then ethylcyclohexane was postdosed for 60 s.

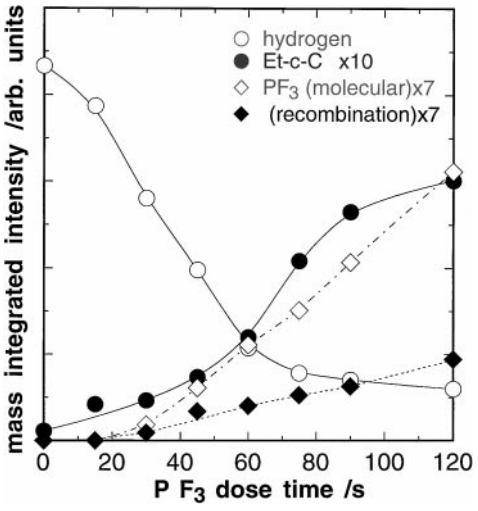

FIG. 3. Dependence of TPD peak areas of PF_3 (PF_2^+, $m/e = 69$), H_2, and ethylcyclohexane ($C_4H_7^+$, $m/e = 55$) on PF_3 dose time. PF_3 was predosed to clean Ni(755) at 123 K, and then ethylcyclohexane was postdosed for 60 s. From the mass balance between hydrogen and ethylcyclohexane, the amount of adsorbed ethylcyclohexane was determined to be 0.013 ± 0.002 ML. The indicated lines are only guides for the eyes.

all the experiments. The TPD spectra for hydrogen desorption (Fig. 2a) were characterized by the presence of two peaks at about 370 and 465 K. Upon an increase in PF_3 dose time, the total peak intensity decreased while the position of the main peak around 370 K shifted slightly from 365 to 375 K. The shape of the higher temperature peak was changed abruptly after a PF_3 dose time of 15 s, though its peak position remained almost unchanged at 465 K with further increases in dose time. For a PF_3 dose time of 120 s, the peak became very broad, extending from 250 to 480 K. The amount of desorbed hydrogen was reduced to that of the hydrogen adsorbed from residual gas. In the presence of a larger amount of coadsorbed PF_3, the peak of desorbed hydrogen became much broader than that of the residual hydrogen adsorption on clean Ni(755), whose peak was located from 350 to 450 K (13).

Figure 2b displays the variations in TPD spectra for ethylcyclohexane ($C_4H_7^+$, $m/e = 55$) with PF_3 dose time and clearly shows the interaction between PF_3 and ethylcyclohexane: (1) in the absence of coadsorbed PF_3, the peak of undecomposed ethylcyclohexane was observed at 253 K; (2) this peak shifted to a lower temperature (218 K) with broadening upon an increase in PF_3 dose time, which indicates the adsorbate–adsorbate interaction between PF_3 and ethylcyclohexane; and (3) after a dose time of 45 s, another sharp peak appeared at 152 K and grew in intensity. The position of this sharp peak was quite similar to that of multilayer ethylcyclohexane (158–162 K), which was observed when only ethylcyclohexane was dosed for >180 s at 123 K, and its peak width was similar to that of multilayer ethylcyclohexane. Therefore, this peak probably came from the ethylcyclohexane adsorbed on the overlayer of adsorbed PF_3. Most of the ethylcyclohexane could not interact with the nickel surface directly in the presence of a larger amount of coadsorbed PF_3, and it became difficult for the decomposition of ethylcyclohexane to proceed. Similar multilayer-like desorption was already observed for the coadsorption of CO and cyclohexane (12) or cycloheptane (13).

Figure 3 shows the dependence of TPD peak areas of PF_3, H_2, and ethylcyclohexane on PF_3 dose time. The amount of desorbed PF_3 in Fig. 3 was smaller by about 5% than that in Fig. 1b at the same dose time. Especially, the recombination peak of PF_3 fragments was not saturated, even by a dose time of 120 s. These results suggest that some part of adsorbed PF_3 and/or PF_3 fragments might react to the hydrogen atoms or hydrocarbon species. Then, we used the coverages of PF_3 estimated in Fig. 1c because PF_3 was predosed to clean Ni(755) also in Figs. 2 and 3. The peak area of hydrogen decreased with an increase in PF_3 dose time and that of ethylcyclohexane increased with an increase in PF_3 dose time. The decomposition of ethylcyclohexane was inhibited almost completely by the presence of coadsorbed $PF_3 > 0.17$ ML (the sites for the recombination peak were saturated with PF_3 by this coverage when exposing only PF_3 for 90 s).

The amount of adsorbed ethylcyclohexane in Fig. 3 (the dose time of ethylcyclohexane = 60 s) was determined to be 0.013 ± 0.002 ML. Since the coverage of ethylcyclohexane used in the coadsorption experiments was much smaller than the saturation coverage of the monolayer (0.05 ML), it is reasonable that the decomposition of PF_3 still occurred in the presence of coadsorbed ethylcyclohexane. The decomposition fraction (ratio of decomposed molecules to adsorbed ones) at zero PF_3 dose time determined was 0.92 ± 0.04. Unlike cyclohexane, whose initial decomposition fraction (decomposition fraction extrapolated to zero coverage of a hydrocarbon) without CO promotion was only 0.1 (12), the initial decomposition fraction of ethylcyclohexane became 1.0 by the introduction of an ethyl group into a cyclohexane ring. As ethylcyclohexane was decomposed efficiently on Ni(755), any promoting effect of coadsorbed PF_3 on the decomposition of ethylcyclohexane was not observed independently of the coverages.

To compare the inhibiting effects between PF_3 and CO, a similar experiment was carried out for the coadsorption of ethylcyclohexane and CO. Figure 4 shows the dependence of TPD peak areas of CO, H_2, and ethylcyclohexane on CO dose time. The peak area of CO increased almost linearly with CO dose time up to 60 s and was nearly saturated after that time. The amount of adsorbed CO in Fig. 4 was similar to that for a clean surface when comparing at the same CO dose time. A desorption peak of CO was observed around 440 K (12), whose position and shape were quite similar to those on Ni(111) reported by others (14, 17). The

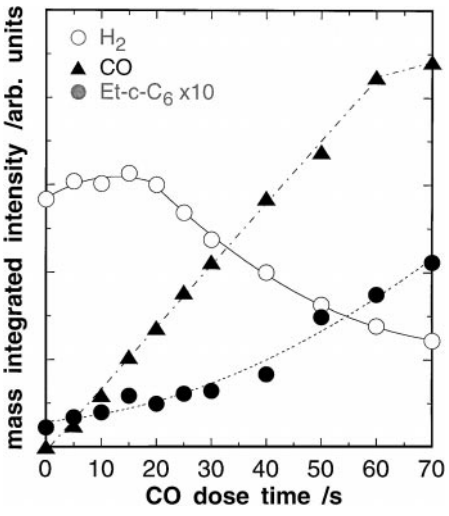

FIG. 4. Dependence of TPD peak areas of CO, H_2, and ethylcyclohexane ($C_4H_7^+$, $m/e = 55$) on CO dose time. Ethylcyclohexane was predosed to clean Ni(755) at 123 K for 75 s, and then CO was postdosed. From the mass balance between hydrogen and ethylcyclohexane, the amount of adsorbed ethylcyclohexane was determined to be 0.017 ± 0.002 ML. The indicated lines are only guides for the eyes.

desorption of CO from Ni(755) occurred at a little higher temperature than the molecular desorption of PF_3 around 350 K (cf. Fig. 1a), which is consistent with the results for Ni(111) (1).

At CO dose time up to 20 s, the peak areas of hydrogen and ethylcyclohexane remained almost constant. With further increasing in dose time, the peak area of hydrogen decreased while that of ethylcyclohexane increased. Decomposition of ethylcyclohexane was inhibited partially by the presence of coadsorbed CO at the coverage >0.2 ML. Even for the coverage around 0.5 ML, coadsorbed CO reduced the decomposition probability of ethylcyclohexane to about half the value without CO while it became nearly zero in the presence of coadsorbed PF_3 >0.17 ML. Thus, the inhibiting effect of CO on decomposition was not so effective as that of PF_3 (cf. Fig. 3). The interaction between CO and ethylcyclohexane was similar to that for PF_3, shown in Fig. 2b. The multilayer-like desorption of ethylcyclohexane was clearly observed only for the coverage >0.4 ML, indicating that a larger amount of coadsorbed species was necessary to produce the multilayer-like desorption of ethylcyclohexane for coadsorption with CO than PF_3. Coadsorbed CO as well as PF_3 did not promote the decomposition of ethylcyclohexane. A similar inhibiting effect of coadsorbed CO was observed for other high-reactivity hydrocarbons such as cycloheptane (13). From the mass balance between hydrogen and ethylcyclohexane in Fig. 4 (the dose time of ethylcyclohexane = 75 s), the amount of adsorbed ethylcyclohexane and the decomposition fraction at zero CO dose time were also determined to be 0.017 ± 0.002 and 0.84 ± 0.04 ML, respectively.

Previously, we have reported a method to determine the decomposition starting temperature of hydrocarbons on a single-crystal surface by taking into consideration the changes in TPD spectra after preflash and postdosing CO (13). The term "decomposition starting temperature" indicates the temperature where an adsorbed hydrocarbon starts to decompose. This method utilizes the inhibiting effect of postdosed CO on the decomposition of a hydrocarbon: i.e., post-dosed CO inhibits the decomposition of a hydrocarbon considerably unless the pre-adsorbed hydrocarbon is dissociated during the preflash step. However, once some dehydrogenated intermediates are produced, postdosed CO cannot inhibit the decomposition of intermediates and then the amount of hydrogen produced from the decomposition of intermediates increases. We have defined the term "decomposition starting temperature" as the temperature where the hydrogen signal begins to increase (13). This method to determine the decomposition starting temperature involved the following four steps: (1) pre-adsorption of a hydrocarbon; (2) brief flash at 10 K/s to a desired temperature, which is termed "preflash temperature" here, to initiate decomposition of an adsorbed hydrocarbon; (3) cooling and postadsorption of CO; and (4) measurement of TPD spectrum. The entire procedure starting from cleaning Ni(755) followed by procedures (1)–(4) was repeated to study another preflash temperature. Figure 5a shows the variations in TPD peak areas of hydrogen and CO with preflash temperature. The results by using PF_3 in the place of CO are displayed in Fig. 5b. The hydrogen signal in Figs. 5a and 5b began to increase around 200 K and reached a constant value by ca. 240 K. In contrast, the decrease in peak areas of CO and recombination peak of PF_3 was observed while the S/N ratio of the data was not as good as the hydrogen signal. These results indicated that the decomposition of ethylcyclohexane to intermediates started at ca. 200 K and finished by 240 K. From the temperature where the hydrogen signal began to increase, the decomposition starting temperature of ethylcyclohexane was determined to be 197 ± 5 K for both cases. The same decomposition starting temperature could be obtained by using the inhibiting effects of both PF_3 and CO. The increasing edge of the hydrogen signal was sharper for the case of PF_3 as PF_3 inhibits the decomposition of ethylcyclohexane more efficiently than CO. As seen in Fig. 5b, the recombination peak of PF_3 decreased when ethylcyclohexane began to decompose to intermediates, whereas the peak area of the molecular desorption of PF_3 stayed almost constant. These results suggest that the produced intermediates inhibited the adsorption and/or dissociation of PF_3 and that the decomposition of both ethylcyclohexane and PF_3 occurred at the step sites of Ni(755).

By the method described above, we have determined the decomposition starting temperature of various saturated hydrocarbons (cyclic and linear ones between C_5 and C_8).

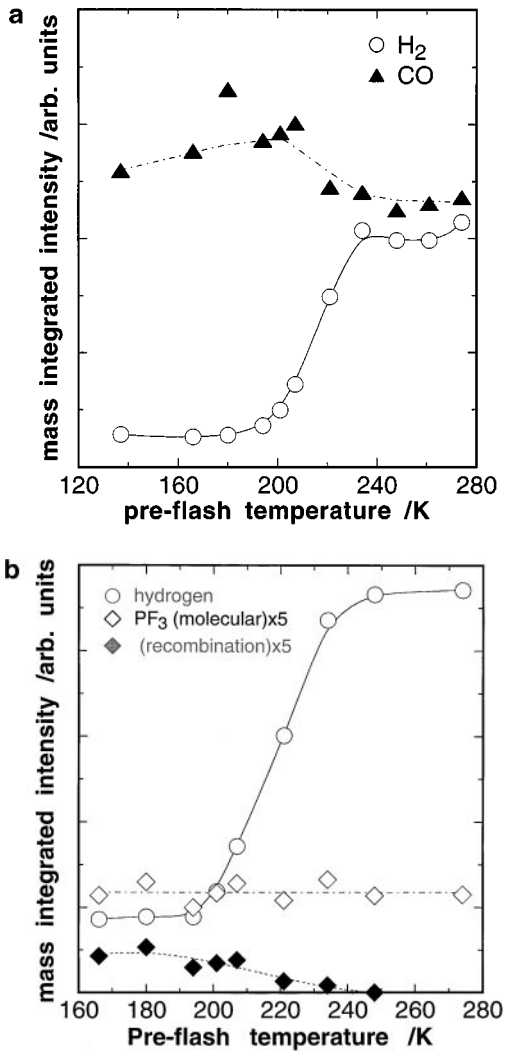

FIG. 5. (a) Variations in TPD peak areas of hydrogen and CO with preflash temperature. Ethylcyclohexane was predosed at 123 K for 60 s (ethylcyclohexane, 0.013 ML), and the surface was flashed at 10 K/s to a preflash temperature to initiate decomposition of ethylcyclohexane. After being cooled to 123 K, CO was postdosed to the surface for 60 s to saturate the surface with CO, and then a TPD spectrum was measured. (b) Variations in TPD peak areas of hydrogen and PF_3 (PF_2^+, $m/e = 69$) with preflash temperature. Ethylcyclohexane was predosed for 60 s, and PF_3 was postdosed for 90 s after the preflash step. The indicated lines are only guides for the eyes.

The detailed results and discussions on the mechanism of hydrocarbon decomposition will be published elsewhere (18).

4. CONCLUSIONS

TPD spectra for the exposure of PF_3 were characterized by two desorption features around 350 and 650 K. The lower temperature desorption feature and the higher one were assigned to the desorption of undecomposed PF_3 and the recombinative desorption of PF_3 fragments, respectively. Decomposition of PF_3 occurs probably at the step sites but not on the terrace of Ni(755). PF_3 inhibited the decomposition of ethylcyclohexane almost completely and the inhibiting effect of PF_3 was more effective than CO. The same decomposition starting temperature of ethylcyclohexane was obtained by using the inhibiting effects of PF_3 as well as CO. The determination of decomposition starting temperature was more exact in the case of PF_3 as PF_3 inhibits the decomposition of ethylcyclohexane more efficiently than CO.

REFERENCES

1. Nitschke, F., Ertl, G., and Kuppers, J., *J. Chem. Phys.* **74**, 5911 (1981).
2. Alvey, M. D., and Yates, J. T., Jr., *J. Am. Chem. Soc.* **110**, 1782 (1988).
3. Dippel, R., Weiss, K.-U., Schindler, K.-M., Woodruff, D. P., Gardner, P., Fritzsche, V., Bradshaw, A. M., and Asensio, M. C., *Surf. Sci.* **287/288**, 465 (1993).
4. Bonzel, H. P., Bradshaw, A. M., and Ertl, G., Eds., "Physics and Chemistry of Alkali Metal Adsorption." Elsevier, Amsterdam, 1989.
5. Hag, S., Love, J. G., and King, D. A., *Surf. Sci.* **275**, 170 (1992). Mitchell, G. E., Gland, J. L., and White, J. M., *Surf. Sci.* **131**, 167 (1983), and references therein.
6. Mate, C. M., and Somorjai, G. A., *Surf. Sci.* **160**, 542 (1985). Blass, P. M., Akhter, S., and White, J. M., *Surf. Sci.* **191**, 406 (1987). Jakob, P., and Menzel, D., *Surf. Sci.* **235**, 15 (1990).
7. Akhter, S., and White, J. M., *Surf. Sci.* **180**, 19 (1987). Henderson, M. A., Mitchell, G. E., and White, J. M., *Surf. Sci.* **203**, 378 (1988).
8. Campbell, C. T., Campbell, J. M., Dalton, P. J., Henn, F. C., Rodriguez, J., and Seimanides, S. G., *J. Phys. Chem.* **93**, 806 (1989), and the three accompanying papers; Domagala, M. E., and Campbell, C. T., *J. Vac. Sci. Technol. A* **11**, 2128 (1993).
9. Sasaki, T., Aruga, T., Kuroda, H., and Iwasawa, Y., *Surf. Sci.* **240**, 223 (1990), and references therein.
10. Jiang, L. Q., Avoyan, A., Koel, B. E., and Falconer, J. L., *J. Am. Chem. Soc.* **115**, 12106 (1993).
11. Zhou, Y., Liu, Z.-M., and White, J. M., *Surf. Sci.* **230**, 85 (1990). Chakarian, V., Shuh, D. K., Yarmoff, J. A., Tao, H.-S., Diebold, U., Maschhoff, B. L., Madey, T. E., and Shinn, N. D., *J. Chem. Phys.* **100**, 5301 (1994). Fan, J., and Trenary, M., *Surf. Sci.* **282**, 76 (1993).
12. Orita, H., Kondoh, H., and Nozoye, H., *Chem. Phys. Lett.* **228**, 385 (1994).
13. Orita, H., Kondoh, H., and Nozoye, H., *J. Phys. Chem.* **99**, 3648 (1995).
14. Trenary, M., Uram, K. J., Bozso, F., and Yates, J. T., Jr., *Surf. Sci.* **146**, 269 (1984).
15. Nozoye, H., *Chem. Lett.* 1429 (1986).
16. Zhou, Y., Mitchell, G. E., Henderson, M. A., and White, J. M., *Surf. Sci.* **214**, 209 (1989).
17. Peebles, D. E., Creighton, J. R., Belton, D. N., and White, J. M., *J. Catal.* **80**, 482 (1983). Surnev, L., Xu, Z., and Yates, J. T., Jr., *Surf. Sci.* **201**, 1 (1988).
18. Orita, H., Kondoh, H., and Nozoye, H., *J. Phys. Chem. B* **104**, 8692 (2000).